Proc. Natl. Acad. Sci. USA
Vol. 94, pp. 412–417, January 1997
Biochemistry

In vitro scanning saturation mutagenesis of an antibody binding pocket

ELIZABETH A. BURKS*, GANG CHEN*, GEORGE GEORGIOU†‡, AND BRENT L. IVERSON*†

*Department of Chemistry and Biochemistry, †Molecular Biology Program, and ‡Department of Chemical Engineering, University of Texas, Austin, TX 78712

Communicated by Allen J. Bard, University of Texas, Austin, TX, November 12, 1996 (received for review September 10, 1996)

ABSTRACT **We have combined PCR mutagenesis with *in vitro* transcription/translation and ELISA for the rapid generation and characterization of antibody mutants. The PCR products are used directly as the template for the *in vitro* transcription/translation reactions and because no cloning steps are required, the *in vitro* saturation mutagenesis of one residue can be completed in duplicate within a week by a single investigator. *In vitro* scanning saturation mutagenesis was used to analyze the role and plasticity of six key contact residues (H:Tyr-33, H:Asn-35, H:Tyr-50, H:Trp-100, L:Val-94, and L:Pro-96) in the binding pocket of a single chain Fv antibody derived from the 26–10 monoclonal antibody. A total of 114 mutant antibodies were produced; all 19 substitutions at each of the 6 chosen positions. The mutants were analyzed for binding to digoxin, digitoxin, digoxigenin, and ouabain resulting in the generation of a comprehensive data base of 456 relative affinity values. Excellent agreement between the relative affinity values obtained with *in vitro* synthesized mutant antibodies and equilibrium affinity data obtained with previously reported purified mutant monoclonal antibodies was observed. Approximately 75% of the single amino acid mutants exhibited significant binding to one or more of the digoxin analogs. Mutations that alter and, in some cases, reverse specificity for the different digoxin analogs were identified. *In vitro* scanning saturation mutagenesis represents a new tool for protein structure-function and engineering studies and can be interfaced with laboratory automation so that an even higher throughput of protein mutants can be constructed and analyzed.**

Structure-guided site-specific mutagenesis represents a powerful tool for the dissection and engineering of protein–ligand interactions (1, 2). One particularly useful mutagenesis technique is alanine scanning mutagenesis in which a number of residues are substituted individually with the amino acid alanine so that the effects of losing side-chain interactions can be determined, while minimizing the risk of large-scale perturbations in protein conformation (3). However, the substitution of functional residues with alanine or any other single amino acid can give misleading results regarding their mechanistic importance (4).

Tremendous attention continues to be focused on antibodies because they define a paradigm of high-affinity protein binding and they are among the most important classes of commercial protein molecules. Antigen binding is determined primarily, but not exclusively, by amino acid residues in the antibody hypervariable or complementarity determining regions I, II, and III of the heavy (H) and light (L) chains. Site-specific mutagenesis and the screening of antibody libraries by phage display have been used to explore the effect of amino acid substitutions on antigen affinity (5–13). Such studies have demonstrated that even antibodies generated from the secondary immune response are not necessarily "optimized" with respect to affinity and/or specificity (10–13). There is evidence that the antigen binding site exhibits a fair degree of plasticity in that a number of amino acid substitutions are tolerated and occasionally improve affinity (6, 12).

Comprehensive information on the functional significance and information content of a given residue of an antibody can best be obtained by saturation mutagenesis in which all 19 amino acid substitutions are examined. The shortcoming of this approach is that the logistics of multiresidue saturation mutagenesis are daunting (4, 14). Hundreds, and possibly even thousands, of site specific mutants must be studied. For each mutant protein, the appropriate gene construct must be made, the DNA must be transformed into a host organism, transformants need to be selected and screened for expression of the protein, the cells have to be grown to produce the protein, and finally the recombinant mutant protein must be isolated. There have been only a handful of studies where one, or at most a few, residues in an antibody have been subjected to saturation mutagenesis. Even in those studies, only some of the mutants were examined in detail (5, 6, 15).

In recent years, techniques for estimating the equilibrium constant for ligand binding using minuscule amounts of protein have been developed (16–18). In this work we have shown that the ability to perform functional assays with small amounts of material can be exploited to develop highly efficient, *in vitro* methodologies for the saturation mutagenesis of antibodies. We have bypassed all time-consuming cloning steps by combining PCR mutagenesis with coupled *in vitro* transcription/translation for the high throughput generation of protein mutants. Here, the PCR products are used directly as the template for the *in vitro* transcription/translation of the mutant single chain antibodies. Because of the high efficiency with which all 19 amino acid substitutions can be generated and analyzed in this way, it is now possible to perform saturation mutagenesis on numerous residues of interest, a process that can be described as *in vitro* scanning saturation mutagenesis.

A high-affinity anti-digoxin single chain Fv (scFv(Dig)) (19) derived from the well-studied anti-digoxin 26–10 murine monoclonal antibody (20) was selected as a model system for our studies. Digoxin and related cardiac glycosides consist of a 5β,14β-steroid body, linked to an α,β-unsaturated lactone at C17 and an O-linked carbohydrate at position 3. The 26–10 antibody binds to the cardiac glycosides digoxin, digitoxin, and digoxigenin with high-affinity ($K_a \approx 9 \times 10^9\ M^{-1}$) and with a 42-fold lower affinity to ouabain (21). The three-dimensional structure of the 26–10 Fab complexed with digoxin (22) reveals that the 3′-tridigitoxose is exposed to the solvent, whereas the lactone ring is fully buried at the bottom edge of the binding site (Fig. 1). Unlike other antibody–antigen complexes (23), binding does not appear to cause detectable conformational changes of either the antibody or the hapten. Both affinity and specificity are derived entirely from shape complementarity,

The publication costs of this article were defrayed in part by page charge payment. This article must therefore be hereby marked "*advertisement*" in accordance with 18 U.S.C. §1734 solely to indicate this fact.

0027-8424/97/94412-6$2.00/0
PNAS is available online at **http://www.pnas.org**.

Abbreviations: H, heavy; L, light.

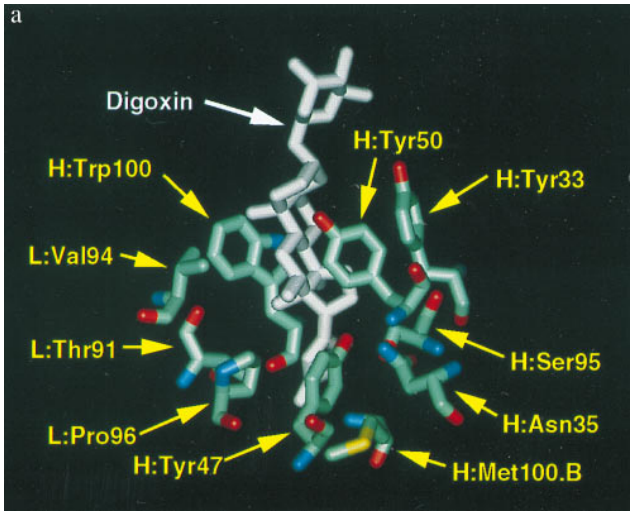

b

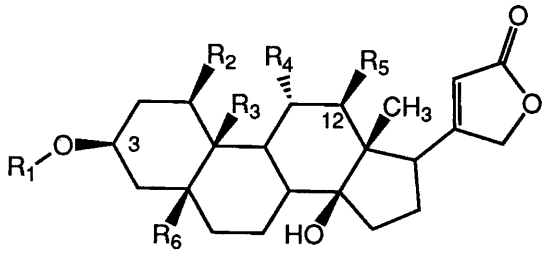

	R_1	R_2	R_3	R_4	R_5	R_6
Digoxin	Sugars	H	CH_3	H	OH	H
Digitoxin	Sugars	H	CH_3	H	H	H
Digoxigenin	H	H	CH_3	H	OH	H
Ouabain	Sugar	OH	CH_2OH	OH	H	OH

FIG. 1. (*a*) Computer model showing bound digoxin and 10 residues that define the 26–10 binding pocket. This figure was generated using Quanta CHARMM software (Micron Separations) using the coordinates of Jeffery *et al.* (22). (*b*) Structures of digoxin and the three analogs used in these studies.

since no hydrogen bonds have been identified between digoxin and the antibody.

In vitro scanning saturation mutagenesis was used to analyze the role and plasticity of six key contact residues in the scFv(Dig). The relative affinities of a total of 114 mutant antibodies for digoxin, digitoxin, digoxigenin, and ouabain were determined resulting in the generation of a comprehensive data base of 456 relative affinity values.

MATERIALS AND METHODS

Taq polymerase was purchased from Promega, dNTPs from Pharmacia, and oligonucleotide primers from Midland Certified Reagent (Midland, TX). Pyruvate kinase, tRNA, and nucleotide triphosphates were obtained from Boehringer Mannheim. Digoxin and digitoxin were purchased from Sigma.

PCR Mutagenesis. Mutations in the scFv(digoxin) antibody were generated by the overlapping PCR method (24–26). Briefly, the plasmid pET25b(scFv(Dig)) (27) was used as a template for PCR. For the first round PCR, a 2-kb *Nde*I–*Pvu*I fragment from pET25b(scFv(Dig)) was used as the 3′ template, whereas a 4-kb *Xho*I–*Pvu*I fragment was used as the 5′ template. The restriction fragments were isolated on an agarose gel to eliminate the possibility that any contaminating full-length, wild-type scFv(Dig) construct was present. A list of the primers used for the first and second PCR steps is available upon request from the authors. First round PCR was carried out in 50 mM KCl, 10 mM Tris·HCl (pH 9.0) at 25°C/0.1% Triton X-100, 0.2 mM dNTPs, 2.5 units *Taq* polymerase (Promega), 0.6 μM each of the two primers, and 0.05 μg template in 100 μl total volume. Amplification was carried out using the following sequence: one cycle at 94°C for 2 min; 29 cycles consisting of 94°C for 1 min, 55°C 2 min, and 72°C for 3 min; one cycle of 94°C for 1 min, 55°C for 2 min, and 72°C for 10 min. The PCR products from the first round were gel-purified and used, together with outside primers, in the overlap extension PCR reaction. For this round of PCR, the mix contained 50 mM KCl, 10 mM Tris·HCl (pH 9.0) at 25°C/0.1% Triton X-100, 0.2 mM dNTPs, 2.5 units *Taq* polymerase (Promega), 0.6 μM each of the two primers, and 0.05 μg each of both the 5′ template and the 3′ template in 100 μl total volume. The amplification sequence for the overlap extension reaction was the same as for the first round reactions except that the annealing temperature for the first five cycles was set between 48°C and 55°C, depending on the melting temperature of overlapping sequence. The PCR products were ethanol precipitated and the pellets were resuspended in 100 μl of water.

***In Vitro* Transcription/Translation.** *In vitro* protein synthesis using an *Escherichia coli* coupled transcription/translation system was carried out essentially as described (28). T7 RNA polymerase and S30 *E. coli* extract for coupled transcription/translation were prepared using standard procedures (28, 29). The coupled transcription/translation reactions were carried out in 30 μl total volume and the reaction mix contained the following: 55 mM Tris acetate (pH 7.8), 2 mM DTT, 1.2 mM ATP, 0.8 mM CTP, 0.8 mM GTP, 0.8 mM UTP, 2% polyethylene glycol (M_r, 8000), 27 mM phospho*enol*pyruvate, 0.4 mM cAMP, 35 μg/ml folinic acid, 30 mM ammonium acetate, 72 mM KOAc, 1.5 mM $Ca(OAc)_2$, 0.35 mM of each amino acid, 0.5 mM EDTA, 0.3 mM glucose 6-phosphate, 2 μg T7 RNA polymerase, 0.4 μg pyruvate kinase, 20 μg tRNA, 5 μg rifampicin, 13.3 mM $Mg(OAc)_2$, and 5 μl of *E. coli* S30 fraction. Reactions were initiated by adding 0.5 μg of the DNA produced by overlap extension in 7 μl. For radiolabeling of the protein synthesis products 0.083 mM of ^{35}S-methionine (1175 Ci/mmol, 1 Ci = 37 GBq; New England Nuclear), was added to the reaction mix. Reactions were incubated for 25 min at 37°C with gentle shaking and were stopped by placing on ice.

General Procedures. SDS/PAGE was carried out in 15% polyacrylamide gels (30). Overlap extension PCR products were sequenced by the dideoxy sequencing method. Representative PCR products were also sequenced following subcloning into pET25b(scFv(Dig)). The digoxin–BSA, digitoxin–BSA, and ouabain–BSA conjugates used in the ELISA analysis were prepared via oxidation of the terminal sugar residues with $NaIO_4$ followed by covalent attachment to BSA through reductive amination in the presence of $NaBH_4$ (31). The digoxigenin–BSA conjugate was prepared from a direct reaction between BSA and 3-aminodeoxydigoxigenin hemisuccinimide (Molecular Probes) according to the manufacturer's instructions.

ELISA. Antibody capture ELISA was performed using standard procedures (32), using 1% (wt/vol) boiled powdered milk (Carnation) as the blocking agent. The plates were washed three times and were developed with the colorimetric horseradish peroxidase substrate 2,2′-azine-bis(3-ethylbenzothiazoline)-6-sulfonic acid diammonium salt (ABTS) (Pierce). The absorbance of each well of the ELISA plates was measured at 405 nm on a microplate autoreader when the ABTS reaction was still in the linear range, a fact that was confirmed by taking several time points per plate. For each cardiac glycoside being investigated (digoxin, digitoxin, digoxigenin, ouabain) the absorbances for each mutant were linearly scaled to that of the wild-type scFv(Dig), which was assigned a value of 1.0, then plotted in the histograms of Fig. 2. Wild-type scFv(Dig) was

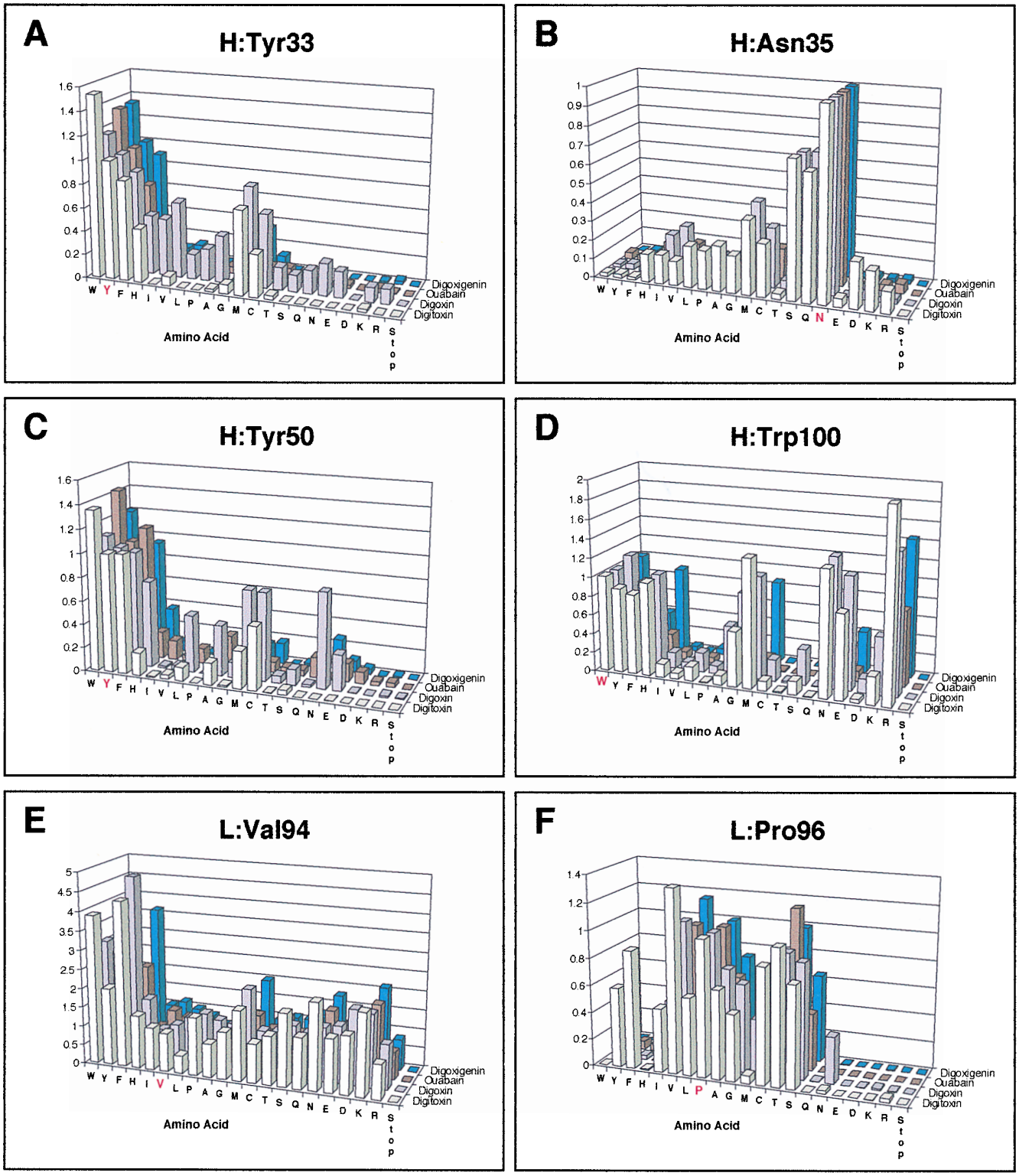

FIG. 2. Histograms of the ELISA data for the different mutant proteins binding to digoxin, digitoxin, digoxigenin, and ouabain. (*A*) Mutations of residue H:Tyr-33. (*B*) Mutations of residue H:Asn-35. (*C*) Mutations of residue H:Tyr-50. (*D*) Mutations of residue H:Trp-100. (*E*) Mutations of residue L:Val-94. (*F*) Mutations of residue L:Pro-96. The plotted values correspond to the absorbance observed in ELISA measured at 405 nm on a microplate autoreader when the ABTS reaction was still in the linear range, a fact that was confirmed by taking several time points per plate. For each cardiac glycoside being investigated (digoxin, digitoxin, digoxigenin, ouabain) the absorbances for each mutant were linearly scaled to that of the wild-type scFv(Dig), which was assigned a value of 1.0, then plotted in the histograms. Wild-type scFv(Dig) was included on every ELISA plate to provide an internal calibration of the data.

included on every ELISA plate to provide an internal calibration for results obtained on different plates. A comprehensive numerical table of the scaled ELISA data is available upon request from the authors.

RESULTS

Our initial *in vitro* scanning saturation mutagenesis studies were performed on six residues that help define the interior of the anti-digoxin 26–10 antibody binding pocket (22). The

single chain Fv form (scFv(Dig)) of the 26–10 antibody was used (19, 27, 33), since the presence of only one polypeptide chain eliminates chain association difficulties that are possible with Fab antibodies. The six chosen 26–10 residues consisted of three aromatic residues that define the largely hydrophobic walls of the binding pocket and thereby make extensive Van der Waals contact with hapten (heavy chain residues H:Tyr-33, H:Tyr-50, and H:Trp-100), a residue that forms hydrogen bonds with contact residues and therefore is presumably of importance in maintaining the architecture of the binding pocket (H:Asn-35) and, finally, two residues that define the bottom of the binding pocket (light chain residues L:Val-94 and L:Pro-96).

For each chosen residue, 21 genes encoding all possible amino acid substitutions, as well as a double stop codon (control), were constructed by overlap extension PCR. All amino acid substitutions were encoded by *E. coli* preferred codons. To eliminate the possibility of contamination with wild-type template, the 3′ and 5′ fragments in the first round PCR were amplified from the respective gel purified restriction fragments as described in *Materials and Methods*. The final products of the overlap extension PCR reaction contain a T7 promoter and ribosome binding site in front of the scFv(Dig) gene. A herpes simplex virus sequence is also present at the end of the scFv(Dig) gene, so that the scFv(Dig) protein can be detected by ELISA using an anti-herpes simplex virus sequence monoclonal antibody.

The PCR overlap extension products were used as templates for coupled *in vitro* transcription/translation reactions to produce functional scFv(Dig) proteins. The same amount of template was used for each coupled *in vitro* transcription/translation reaction. An *E. coli* S30 ribosomal extract, as opposed to mammalian or plant cell extracts, was used for *in vitro* translation because the bacterial system has the significant advantage of eliminating the need to cap the message. The reactions were run on a 30 μl scale for 25 min at 37°C. Preliminary experiments established that the reaction is completed after 25 min (29). SDS/PAGE autoradiography, Western blots, and hot trichloroacetic acid precipitation of the translation products labeled with [^{35}S]methionine all demonstrated that similar concentrations of polypeptide, ≈10 nM judging from ELISA comparison to an authentic sample of wild-type scFv, are produced in the different transcription/translation reactions using the above protocol, irrespective of the amino acid substitution (29).

The protein products from the coupled *in vitro* transcription/translation step were analyzed by ELISA. Briefly, 96-well microtiter plates were coated with the BSA conjugate of digoxin, digitoxin, digoxigenin, or ouabain. The microtiter plates were then incubated with equal amounts from each of the *in vitro* synthesis reactions. To provide accurate calibration, the construct prepared with the wild-type sequence was used on each ELISA plate. It should be noted that the wild-type construct was produced by the overlapping PCR method alongside the mutants, thereby providing an accurate calibration for all stages of the procedure.

Because of the large number of samples involved in the *in vitro* saturation mutagenesis experiments, several ''quality control'' tests were conducted at key points. Specifically: (*i*) A gel of the PCR products was run prior to the coupled *in vitro* transcription/translation reactions. This analysis confirmed that the correct size products had been produced and also enabled determination of the amount of amplified DNA template to be used in the *in vitro* protein synthesis step. (*ii*) [^{35}S]Methionine was added to the translation mixture and the protein products were analyzed by SDS/PAGE and autoradiography. Western blots were also used to analyze the protein products, using an anti-herpes simplex virus monoclonal antibody for detection. Protein products of the appropriate length and in similar quantities were observed for the different reactions. (*iii*) As mentioned previously, a control reaction that places two adjacent stop codons at the position being mutagenized was carried out every time. Two adjacent stop codons were used to eliminate possible readthrough. Autoradiography of the *in vitro* protein synthesis products confirmed that only truncated polypeptides of the anticipated molecular weight were detected in these control reactions. The truncated scFv(Dig) polypeptides generated by stop codon insertion exhibit no hapten binding and were thus used to establish the baseline in the ELISA assays. (*iv*) For each residue, the entire process was carried out in at least two independent runs to verify the reproducibility of the results. In addition, each ELISA was run in duplicate. Using the protocols described, the reproducibility of the data was excellent with absorbance values >20% of wild-type, varying by no more than ±5% between experiments (performed by different investigators). ELISA values lower than 20% of wild type exhibited a greater degree of variability, presumably because of the lower signal-to-noise ratio. A low or absent ELISA signal means that the off-rate is too fast for the scFv(Dig) mutants to remain bound to a significant extent during the incubations and washing steps, but does not necessarily imply complete loss of binding.

The ELISA results for the different mutants binding to digoxin and the three analogs (456 relative affinity values in all) are plotted as histograms in Fig. 2. All absorbance values are normalized to the wild-type construct to allow for direct comparisons. Schildbach *et al.* (21) have reported that the relative digoxin:digitoxin, digoxin:digoxigenin, and digoxin :ouabain affinities are 2:1, 1:1, and 42:1, respectively. Therefore, the relative ELISA values for the different cardiac glycosides in Fig. 2 *A–F* must be scaled accordingly before any direct comparisons are made.

DISCUSSION

A striking feature of the data shown in Fig. 2 is that 86 of the 114 substitutions in residues H:Tyr-33, H:Asn-35, H:Tyr-50, H:Trp-100, L:Val-94, or L:Pro-96 result in significant (>15% of wild-type) recognition and binding to one or more of the digoxin analogs. The large number of amino acid substitutions that can be tolerated is highly indicative of the plasticity of the antigen binding site. Other studies have also indicated that single amino acid mutations in the complementarity determining regions generally do not abolish binding to haptens (6, 7). Chen and colleagues have suggested that the ability of antibody genes to tolerate single amino acid mutations is of significance for somatic hypermutation because it allows mutated B lymphocytes to remain functional while undergoing further affinity maturation (6).

None of the amino acid replacements of L:Val-94 abolishes antigen binding. This result is probably related to the fact that in the crystal structure the side chain of L:Val-94 does not directly contact digoxin (22). Several substitutions at L:94 gave a higher absorbance reading in the ELISA assays compared with wild-type valine. A higher ELISA signal can result either from improved binding affinity, more efficient folding, or avidity effects due to dimerization. The latter is not likely in this case because the scFv(Dig) concentrations produced by *in vitro* translation are low, making dimerization highly unfavorable. It is not possible to distinguish from the ELISA alone between mutants that fold more efficiently and those having a higher affinity for the hapten. Nevertheless, it is noteworthy that in the case of L:Val-94 mutants, the highest absorbance values (Fig. 2*E*) were observed with aromatic amino acid substitutions that should result in a larger hapten contact area. Hydrophobic substitutions such as L:Val-94-Phe, L:Val-94-Trp, or L:Val-94-Tyr could presumably improve digoxin binding relative to the wild-type scFv(Dig) antibody by making additional Van der Waals contacts. Regardless of the detailed explanation, our results emphasize that not all residues are

optimized in even high-affinity antibodies such as 26–10, and that the absence of close contact with the hapten confers higher plasticity, i.e., the ability to tolerate a wider range of substitutions without compromising binding.

High-affinity scFv(Dig) mutants selected by fluorescence-activated cell sorting from a library displayed on the surface of *E. coli* (33) had predominantly aromatic substitutions at L:Val-94 (P. Daugherty, G.C., B.L.I., and G.G., unpublished work). The high representation of aromatic residues in clones selected from a library is consistent with the increased hapten binding data of the respective *in vitro* synthesized clones.

For the three heavy chain aromatic residues that make substantial Van der Waals contacts with bound digoxin, H:Tyr-33, H:Tyr-50, and H:Trp-100, conservative changes to any of the other aromatic amino acids largely retained or slightly improved the ELISA signal and there was little effect on specificity. The smaller, more polar histidine was tolerated noticeably less well than the other aromatic amino acids, supporting the notion that hydrophobic contact surface area is important in these positions. Methionine retained substantial activity in all three cases, a fact that is consistent with a ranking of this amino acid close to the large aromatic amino acids in both size and hydrophobicity indices (34). However, it is important to note that large aromatic amino acids are not essential for binding at any one of the positions (H:33, H:50, or H:100). Substitution of Asn for H:Tyr-50 or H:Trp-100 had only a slight effect on digoxin binding, but diminished activity was observed when substituted for H:Tyr-33. Somewhat surprisingly, the positively charged residues lysine and arginine retained partial and full digoxin binding activity, respectively, when substituted for H:Trp-100. It is noteworthy that the highest affinity mutant isolated from a heavy chain library in which H:Trp-100 was mutagenized also had an arginine at H:100 (P. Daugherty, unpublished work).

Our results with H:Asn-35 are consistent with this residue playing largely a structural role in the scFv(Dig) binding pocket owing to specific hydrogen bonds to H:Tyr-47, as well as the H:Ser-95 that were identified in the crystal structure of 26–10 (22). The most active replacements for H:Asn-35, namely H:Asn-35Gln and H:Asn^{35}Ser, have side chains that also can potentially take part in hydrogen bonding.

In general, digoxigenin binding correlated with digoxin binding, a fact that is consistent with the minimal role that the sugar moieties appear to play in the binding of digoxin by the 26–10 antibody (22). Moreover, out of the 114 mutants examined, none displayed significantly enhanced affinity for ouabain relative to the other derivatives. Ouabain is larger than the other cardiac glycosides examined and is not accommodated as well in the binding pocket of 26–10 as evidenced by the lower affinity (21). Therefore, an increase in ouabain specificity relative to digoxin should require extensive alterations of the binding site that are not feasible within the context of single amino acid substitutions. On the other hand, a significant change in specificity for digitoxin versus digoxin was observed with certain mutants. For example, L:Pro-96-Tyr or especially L:Pro-96-Phe mutants exhibit binding to digitoxin comparable to wild-type scFv(Dig), whereas binding to digoxin was substantially diminished. The crystal structure (22) indicates that L:Pro-96 is adjacent to the C12 hydroxyl of digoxin, which is absent in digitoxin (Fig. 1). Computer modeling suggests that side chains having smaller volume are capable of accommodating both digoxin and digitoxin. However, digoxin binding is sterically hindered by the larger side chains of L:Pro-96-Phe or L:Pro-96-Tyr, whereas digitoxin binding is not. In agreement with this explanation, the other two molecules with hydroxyl groups at C12, namely ouabain and digoxigenin, also exhibit no binding with the L:Pro-96-Phe and L:Pro-96-Tyr mutants. In the case of L:Pro-96-Trp it appears that the indole ring of tryptophan abolishes binding to any of the haptens either because it causes a large perturbation in the binding pocket or it is simply too large to accommodate even the C12 hydrogen of digitoxin.

Mutants are also observed that retain high affinity for digoxin, while exhibiting substantially decreased binding to digitoxin. Noteworthy examples include several mutants of H:Tyr-33, such as H:Tyr-33-Ile or H:Tyr-33-Asn, and especially H:Tyr-50-Asn. It is unclear from the crystal structure why these residues, which are far from the C12 position of bound digoxin, have such a strong influence on the specificity of digoxin versus digitoxin binding.

There is excellent agreement between the values for relative affinities and specificities for the different digoxin mutants in the literature (12, 21, 35, 36) and the data in Fig. 2. For example, Schildbach *et al.* (21) prepared and analyzed several H:Tyr-50 mutants of the 26–10 IgG. The relative order of digoxin affinities measured by Schildbach *et al.* listed from highest to lowest affinity, for the different H:Tyr-50 mutants was as follows: H:Tyr-50 (wild type) $\sim$ H:Tyr-50-Trp $\sim$ H:Tyr-50-Phe $>$ H:Tyr-50-Asn $>$ H:Tyr-50-His $>$ H:Tyr-50-Leu $>$ H:Tyr-50-Ala $>$ H:Tyr-50-Gly and H:Tyr-50-Asp (34). The H:Tyr-50-Asn and H:Tyr-50-Asp mutants were reported to have increased specificity in favor of digoxin over digitoxin binding. Similarly, Near *et al.* (36) produced and measured the relative affinities for certain H:Asn-35 mutants. The reported order of affinities are H:Asn-35 (wild type) $>$ H:Asn-35-Gln $>$ H:Asn-35-Val $>$ H:Asn-35-Thr $>$ H:Asn-35-Leu $>$ H:Asn-35-Ala and H:Asn-35-Asp (36). Comparison of these data with Fig. 2 reveals good agreement with our ELISA results. Such agreement indicates that the folding efficiencies for the different scFv(Dig) mutants in our experiments, at least those mentioned above, must be comparable so that the ELISA signals reflect primarily the relative affinities of the different mutants. Moreover, it underscores the validity of our methodology for the rapid generation and characterization of mutant antibodies. Finally, comparison of the literature values for the lower affinity mutants and our ELISA measurements place an approximate limit of between 10^6 and 10^7 M^{-1} for the lowest affinity observable in our ELISAs.

It is possible that as *in vitro* scanning saturation mutagenesis is applied to other proteins, or even perhaps other residues of scFv(Dig), there will be instances where certain mutations may affect the concentration of correctly folded protein obtained by *in vitro* transcription/translation, thereby prohibiting the interpretation of the ELISA results solely on the basis of antigen affinity. Even in the case when an ELISA signal does not indicate a difference in affinity, ELISA readings substantially higher than wild-type are of interest since they identify residues that facilitate higher levels of expression or correct folding, critical issues in the large scale expression of scFv antibodies for practical purposes.

As we have demonstrated in this report, *in vitro* scanning saturation mutagenesis provides a rapid method for obtaining a large amount of structure-function information including: (*i*) identification of residues that modulate ligand binding specificity, (*ii*) a better understanding of ligand binding based on the identification of those amino acids that retain activity and those that abolish activity at a given location, (*iii*) an evaluation of the overall plasticity of an active site or protein subdomain, (*iv*) identification of amino acid substitutions that result in increased binding.

The *in vitro* saturation mutagenesis of one residue can be completed in duplicate within a week by a single investigator. In addition, several of the steps are amenable to robotic automation, which could increase the throughput of mutants studied even further. *In vitro* scanning saturation mutagenesis should prove particularly valuable for protein engineering studies, even with enzymes when coupled to a catalytic assay, as a rapid way of identifying mutants with interesting properties that can then be produced in bacteria and subjected to more detailed structural and functional characterization. In

addition, *in vitro* scanning saturation mutagenesis represents a systematic new tool for exploring *in vitro* antibody affinity evolution, analogous to somatic hypermutation *in vivo*. In particular, interesting single mutants could be used as a starting point for subsequent rounds of saturation mutagenesis, so that multiple mutations with additive effects on binding could be identified. This same sequential mutation approach should be useful with other types of proteins, so that attributes such as expression level, folding ability, catalytic rate or substrate specificity could be modulated in a systematic way.

We are grateful to Patrick Daugherty and Dr. Boyd Hardesty for reading the manuscript. This work was supported by Grant NSF BES 94-2502 to B.L.I. and G.G.

1. Wells, J. A. (1996) *Proc. Natl. Acad. Sci. USA* **93,** 1–6.
2. Braisted, A. C. & Wells, J. A. (1996) *Proc. Natl. Acad. Sci. USA* **93,** 5688–5692.
3. Cunningham, B. C., Jhurani, P., Ng, P. & Wells, J. A. (1989) *Science* **243,** 1330–1336.
4. Warren, M. S., Marolewski, A. E. & Benkovic, S. J. (1996) *Biochemistry* **35,** 8855–8862.
5. Ito, W., Iba, Y. & Kurosawa, Y. (1993) *J. Biol. Chem.* **268,** 16639–16647.
6. Chen, C., Robert, V. A., Stevens, S., Brown, M., Stenzel-Poore, M. P. & Rittenberg, M. B. (1995) *EMBO J.* **14,** 2784–2794.
7. Brown, M., Rittenberg, M. B., Chen, C. & Roberts, V. A. (1996) *J. Immunol.* **156,** 3285–3291.
8. Harrison, J. L., Williams, S. C., Winter, G. & Nissim, A. (1996) *Methods Enzymol.* **267,** 109–115.
9. Burton, D. R. & Barbas, C. F., III (1994) *Adv. Immunol.* **57,** 191–280.
10. Yelton, D. E., Rosk, M. J., Cruz, G., Cosand, W. L., Bajorath, J., Hellstrom, I., Hellstrom, K. E., Huse, W. D. & Glaser, S. M. (1995) *J. Immunol.* **155,** 1994–2004.
11. Jackson, J. R., Sathe, G., Rosenberg, M. & Sweet, R. (1995) *J. Immunol.* **154,** 3310–3319.
12. Short, M. K., Jeffery, P. D., Kwong, R.-F. & Margolies, M. N. (1995) *J. Biol. Chem.* **270,** 28541–28550.
13. Wong, Y. W., Kussie, P. H., Parhami-Seren, B. & Margolies, M. N. (1995) *J. Immunol.* **154,** 3351–3358.
14. Hilton, D. J., Watowich, S. S., Katz, L. & Lodish, H. F. (1996) *J. Biol. Chem.* **271,** 4699–4708.
15. Brummell, D. A., Sharma, V. P., Anand, N. N., Bilous, D., Dubuc, G., *et al*. (1993) *Biochemistry* **32,** 1180–1187.
16. Parker, C. W. (1978) in *Handbook of Experimental Immunology*, ed. Weir, D. M. (Blackwell Scientific, Oxford), 3rd Ed.
17. Blackburn, G. F., Shah, H. P., Kenten, J. H., Leland, J., Kamin, R. A., Link, J., Peterman, J., Powell, M. J., Shah, A., Talley, D. B., Tyagi, S. K., Wilkins, E., Wu, T. G. & Massey, R. J. (1991) *Clin. Chem.* **37,** 1534–1539.
18. Bard, A. J. & Whitsides, G. (1993) U.S. Patents 5,221,605 and 5,238,808.
19. Huston, J. S., Levinson, D., Mudgett-Hunter, M., Tai, M.-S., Novotny, J. S., Margolies, M. N., Ridge, R. J., Bruccoleri, R. E., Haber, E., Crea, R. & Opperman, H. (1988) *Proc. Natl. Acad. Sci. USA* **85,** 5879–5883.
20. Mudgett-Hunter, M., Margolies, M. N., Ju, A. & Haber, E. (1982) *J. Immunol.* **129,** 1165–1172.
21. Schildbach, J. F., Near, R. I., Bruccoleri, R. E., Haber, E., Jeffery, P. D., Ng, S.-C., Novotny, J., Sheriff, S. & Margolies, M. N. (1993) *J. Biol. Chem.* **268,** 21739–21747.
22. Jeffery, P. D., Strong, R. K., Sieker, L. C., Chang, C. Y. Y., Campbell, R. L., Petsko, G. A., Haber, E., Margolies, M. N. & Sheriff, S. (1993) *Proc. Natl. Acad. Sci. USA* **90,** 10310–10314.
23. Braden, B. C. & Poljak, R. J. (1995) *FASEB J.* **9,** 9–16.
24. Ho, S. N., Hunt, H. D., Horton, R. M., Pullen, J. K. & Pease, L. R. (1989) *Gene* **77,** 51–59.
25. Horton, R. M. & Pease, L. R. (1991) in *Directed Mutagenesis: A Practical Approach*, ed. McPherson, M. J. (Oxford Univ. Press, New York), pp. 217–247.
26. Higuchi, R., Krummel, B. & Saiki, R. K. (1988) *Nucleic Acids Res.* **16,** 7351–7367.
27. Burks, E. A. & Iverson, B. L. (1995) *Biotechnol. Prog.* **11,** 112–114.
28. Kudlicki, W., Odom, O. W., Kramer, G. & Hardesty, B. (1994) *J. Biol. Chem.* **269,** 16549–16553.
29. Burks, E. A. (1996) Ph.D. thesis (University of Texas, Austin).
30. Laemmli, U. K. (1970) *Nature (London)* **227,** 680–685.
31. Smith, T. W., Bulter, V. P., Jr., & Haber, E. (1970) *Biochemistry* **9,** 331–337.
32. Harlow, E. & Lane, D. (1988) *Antibodies: A Laboratory Manual* (Cold Spring Harbor Lab. Press, Plainview, NY).
33. Francisco, J. A., Campbell, R., Iverson, B. L. & Georgiou, G. (1993) *Proc. Natl. Acad. Sci. USA* **90,** 10444–10448.
34. Tomii, K. & Kanehisa, M. (1996) *Protein Eng.* **9,** 27–36.
35. Schildbach, J. F., Shaw, S.-Y., Bruccoleri, R. E., Haber, E., Herzenberg, L. A., Jager, G. C., Jeffery, P. D., Panka, D. J., Parks, D. R., Near, R. I., Novotny, J., Sheriff, S. & Margolies, M. N. (1994) *Protein Sci.* **3,** 737–749.
36. Near, R. I., Mudgett-Hunter, M., Novotny, J., Bruccoleri, R. & Ng, S. C. (1993) *Mol. Immunol.* **30,** 369–377.